DEVELOPMENT OF A STRAPDOWN INERTIAL NAVIGATION SYSTEM SIMULATION PLATFORM

Dah-Jing Jwo
Department of Communications, Navigation and Control Engineering, National Taiwan Ocean University, Keelung, Taiwan, R.O.C, djjwo@mail.ntou.edu.tw

Jyun-Han Shih
Department of Communications, Navigation and Control Engineering, National Taiwan Ocean University, Keelung, Taiwan, R.O.C

Chia-Sheng Hsu
Department of Communications, Navigation and Control Engineering, National Taiwan Ocean University, Keelung, Taiwan, R.O.C

Kai-Lun Yu
Systems & Technology Corp., New Taipei City, Taiwan, R.O.C

Follow this and additional works at: https://jmstt.ntou.edu.tw/journal

Part of the Controls and Control Theory Commons

DEVELOPMENT OF A STRAPDOWN INERTIAL NAVIGATION SYSTEM SIMULATION PLATFORM

Acknowledgements

DEVELOPMENT OF A STRAPDOWN INERTIAL NAVIGATION SYSTEM SIMULATION PLATFORM

Dah-Jing Jwo[1], Jyun-Han Shih[1], Chia-Sheng Hsu[1], and Kai-Lun Yu[2]

ABSTRACT

This paper presents a strapdown inertial navigation system (SINS) simulation platform. The numerical simulator solves the navigation equations in navigation frame where the quaternion vector is employed for attitude calculation. The measured quantities (angular body rates and specific force) are generated by the numerical simulator. The results are also confirmed with the navigation solutions given by a commercial inertial navigation system toolbox using the generated body angular rates and specific force of the SINS. The paper can provide the readers with further information for developing their own SINS simulation tools.

I. INTRODUCTION

The strapdown inertial navigation system (SINS) [2, 5, 7, 10, 11] has been widely used for positioning and navigation. One of the characteristics of the SINS is that there is no entity platform and the computer is used to complete the function of navigation platform using the so-called mathematical platform.

The measuring devices of SINS, gyroscopes and accelerometers, measure the data along the direction of three-axis system in which the navigation system is installed. Since they are directly tied up in moving vehicles, what they measure are physical data in the body frame. The data needs to be transformed to inertial frame and the key point of the conversion is to calculate real-time attitude to provide mathematical platform, which is called attitude matrix or direction cosine matrix. Attitude updating is an important part of SINS and two of the popular algorithms, i.e., the Euler angle based transformation

and the quaternion approach, are provided.

Working with actual inertial equipment and data is good but problem exists. Often the process of interfacing with equipment and performing data collection can consume more time than the development and execution of the algorithms. It is apparent that the ability to simulate the process on a desktop computer would be helpful indeed.

The objective of this paper is to present a step-by-step development procedure for simulating the SINS. Some of the results are compared to those in the commercial software, Inertial Navigation System Toolbox (INS Toolbox) by GPSoft LLC [3], for validation.

II. COORDINATE SYSTEMS

The following coordinate frames [3, 4, 11, 12] are commonly used in the strapdown inertial navigation systems.

(1) The body frame (b-frame): the b-frame (Fig. 1) is an orthogonal axis set which has its origin located at the center of the vehicle, and is aligned with the pitch x_b axis, roll y_b axis, and yaw z_b axis of the vehicle in which the navigation system is installed.

(2) The inertial frame (i-frame): the i-frame (Fig. 2) has its origin located at the center of the Earth and its axes non-rotating with respect to fixed stars. These axes are denoted by x_i, y_i, and z_i, with z_i being coincident with the Earth polar axis.

(3) The Earth frame (e-frame): the e-frame (Fig. 2) has its origin at the center of the Earth and axes non-rotating with respect to the Earth. These axes are denoted by x_e, y_e, and z_e, where the axis z_e is the Earth polar axis; the axis x_e is along the intersection of the plane of the Greenwich meridian and the Earth equatorial plane; the Earth frame rotates with respect to the inertial frame at a rate ω_{ie} about the axis z_i.

(4) The navigation frame (n-frame): the n-frame (Fig. 2) is a local geographic navigation frame which has its origin at the location of the navigation system, point P (The navigation system is fixed inside the vehicle and it is assumed that the navigation system is located exactly at the center
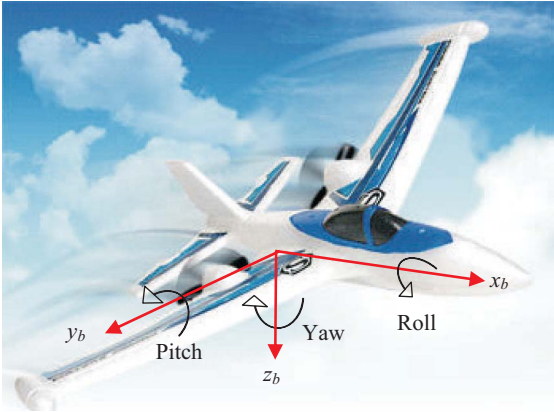
Fig. 1. The body frame illustration and definition of axis rotation [12].
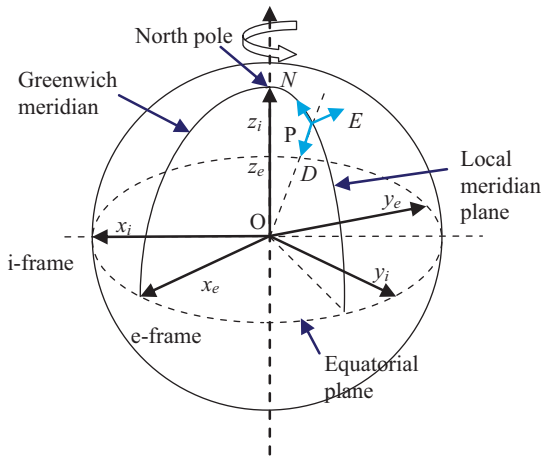

Fig. 2. The reference frames [12].

of the vehicle), and axes aligned with the directions of east, north and the local vertical down. When defined in this way, the n-frame is called the 'NED-frame'. The turn rate of the navigation frame with respect to the Earth-fixed frame, $\boldsymbol{\omega}_{en}$, is governed by the motion of the point P with respect to the Earth. This is often referred to as the transport rate.

III. THE NED-FRAME MECHANIZATION OF STRAPDOWN INERTIAL NAVIGATION SYSTEM

The velocity derivative expressed in the local-level frame is given by [1, 4]

$$\dot{\mathbf{V}}^n = \mathbf{C}_b^n \mathbf{f}^b - [\boldsymbol{\Omega}(\boldsymbol{\omega}_{en}^n) + 2\boldsymbol{\Omega}(\boldsymbol{\omega}_{ie}^n)]\mathbf{V}^n + \mathbf{g}_l^n \qquad (1)$$

where the kinematic velocity is

$$\mathbf{V}^n = [V_N \quad V_E \quad V_D]^T \qquad (2)$$

To solve Eq. (1) the velocity components and Euler's angles of a vehicle should be available as functions of time and their first derivatives should be computed. The velocity components and Euler's angles and their derivatives are used as input for the simulator. In addition, the angular rate vectors ($\boldsymbol{\omega}_{en}^n$ and $\boldsymbol{\omega}_{ie}^n$) and the gravity vector should be computed:

$$\boldsymbol{\omega}_{en}^n = \begin{bmatrix} \dot{\lambda}\cos\varphi \\ -\dot{\varphi} \\ -\dot{\lambda}\sin\varphi \end{bmatrix} = \begin{bmatrix} \dfrac{V_E}{R_M + h} \\ -\dfrac{V_N}{R_N + h} \\ -\dfrac{V_E \tan\varphi}{R_N + h} \end{bmatrix} \qquad (3)$$

$$\boldsymbol{\omega}_{ie}^n = \begin{bmatrix} \omega_{ie}\cos\varphi \\ 0 \\ -\omega_{ie}\sin\varphi \end{bmatrix} \qquad (4)$$

The specific force vector expressed in *b* frame computed by Eq. (1) can be transformed to *n* frame using the direction cosine transformation matrix (DCM). The transformations between the two coordinate frames are written as

$$\mathbf{f}^b = \mathbf{C}_n^b \mathbf{f}^n ; \ \mathbf{f}^n = \mathbf{C}_b^n \mathbf{f}^b \qquad (5)$$

where $\mathbf{f}^n$ and $\mathbf{f}^b$ represent the vectors expressed in the local level navigation coordinate and body coordinate, respectively. It should be noted that the following relation holds

$$\mathbf{C}_b^n = (\mathbf{C}_n^b)^{-1} = (\mathbf{C}_n^b)^T$$

Mathematically the absolute angular velocity is determined by summing the angular velocity of the *b* frame relative to *n* frame $\boldsymbol{\omega}_{nb}$ and the angular velocity of *n* frame relative to *i* frame $\boldsymbol{\omega}_{in}$:

$$\boldsymbol{\omega}_{ib} = \boldsymbol{\omega}_{in} + \boldsymbol{\omega}_{nb} \qquad (6)$$

The body angular velocity relative to the *n* frame $\boldsymbol{\omega}_{nb}$ with components in *b* frame is given by

$$\boldsymbol{\omega}_{nb}^b = \boldsymbol{\omega}_{ib}^b - \mathbf{C}_n^b \boldsymbol{\omega}_{in}^n \qquad (7)$$

where

$$\boldsymbol{\omega}_{in}^n = \boldsymbol{\omega}_{ie}^n + \boldsymbol{\omega}_{en}^n \qquad (8)$$

The relative angular velocity of the *b* frame to the *n* frame is related to the angular rates of Euler's angles as follows:
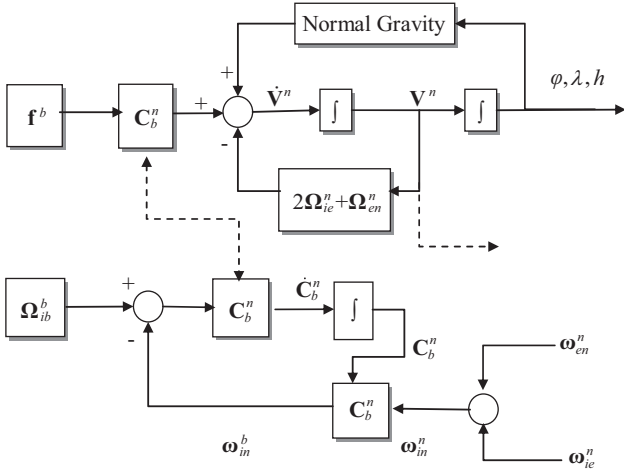
Fig. 3. Block diagram of the strapdown inertial navigation system mechanization expressed in the local-level frame.

$$\boldsymbol{\omega}_{nb}^b = \begin{bmatrix} p \\ q \\ r \end{bmatrix} = \begin{bmatrix} \dot{\Phi} - \dot{\psi}\sin\theta \\ \dot{\theta}\cos\Phi + \dot{\psi}\cos\theta\sin\Phi \\ \dot{\psi}\cos\theta\cos\Phi - \dot{\theta}\sin\Phi \end{bmatrix} \tag{9}$$

The inverse transformation is defined by inversion to be

$$\begin{bmatrix} \dot{\Phi} \\ \dot{\theta} \\ \dot{\psi} \end{bmatrix} = \begin{bmatrix} 1 & \tan\theta\sin\Phi & \tan\theta\cos\Phi \\ 0 & \cos\Phi & -\sin\Phi \\ 0 & \sin\Phi/\cos\theta & \cos\Phi/\cos\theta \end{bmatrix} \begin{bmatrix} p \\ q \\ r \end{bmatrix} \tag{10}$$

where $\mathbf{C}_n^b$ is the transformation matrix related b frame relative to n frame; $\boldsymbol{\omega}_{in}^n$ is the angular velocity column vector of n frame relative to i frame expressed in n frame; p, q, r are standard symbols for, respectively, the roll, pitch, and yaw rate components of the aircraft angular-velocity vector.

The general block diagram of the strapdown inertial navigation system mechanization expressed in the local-level frame is shown in Fig. 3. The toolbox allows one to simulate the vehicle dynamics, raw measurements (delta-V's from the accelerometers and delta-theta's from the gyros) and the data processing. For a vector $\boldsymbol{\omega} = [\omega_x\ \omega_y\ \omega_z]^T$, its corresponding skew symmetric matrix $\boldsymbol{\Omega}$ is written as

$$\boldsymbol{\Omega} = \begin{bmatrix} 0 & -\omega_z & \omega_y \\ \omega_z & 0 & -\omega_x \\ -\omega_y & \omega_x & 0 \end{bmatrix} \tag{11}$$

Calculation of Latitude φ, Longitude λ, Altitude h are carried out using

$$\dot{\varphi} = \frac{V_N}{R_M + h}$$

$$\dot{\lambda} = \frac{V_E}{(R_N + h)\cos\varphi}$$

$$\dot{h} = -V_D \tag{12}$$

which can be written in a more compact form

$$\dot{\boldsymbol{\gamma}}^n = \mathbf{D}^{-1}\mathbf{V}^n \tag{13}$$

where $\boldsymbol{\gamma}^n = [\varphi\ \ \lambda\ \ h]^T$ and

$$\mathbf{D}^{-1} = \begin{bmatrix} \dfrac{1}{R_M + h} & 0 & 0 \\ 0 & \dfrac{1}{(R_N + h)\cos\varphi} & 0 \\ 0 & 0 & -1 \end{bmatrix}$$

The attitude updating algorithm is performed according to the following differential equation

$$\dot{\mathbf{C}}_b^n = \mathbf{C}_b^n(\boldsymbol{\Omega}_{ib}^b - \boldsymbol{\Omega}_{in}^b) = \mathbf{C}_b^n\boldsymbol{\Omega}_{nb}^b$$

The navigation equations for the strapdown inertial navigation system expressed in the local-level frame is given by

$$\begin{bmatrix} \dot{\boldsymbol{\gamma}}^n \\ \dot{\mathbf{V}}^n \\ \dot{\mathbf{R}}_b^n \end{bmatrix} = \begin{bmatrix} \mathbf{D}^{-1}\mathbf{V}^n \\ \mathbf{C}_b^n\mathbf{f}^b - (2\boldsymbol{\Omega}_{ie}^n + \boldsymbol{\Omega}_{en}^n)\mathbf{V}^n + \mathbf{g}_l^n \\ \mathbf{C}_b^n(\boldsymbol{\Omega}_{ib}^b - \boldsymbol{\Omega}_{in}^b) \end{bmatrix} \tag{14}$$

There are two popular types of transformation [3, 6, 8, 9] approaches commonly used in INS applications.

(1) The Euler angle based transformation: As introduced before, the DCM is employed as a transition matrix to describe the transformation of a vector quantity defined in the body frame (denoted by 'b') to the geodetic frame (denoted by 'n'), $\mathbf{f}^n = \mathbf{C}_b^n\mathbf{f}^b$. The two coordinates are related using a vehicle body-to-navigation frame DCM, $\mathbf{C}_b^n$, which can be constructed in terms of the Euler's angles or the quaternion parameters.

$$\mathbf{C}_b^n = \begin{bmatrix} C_\theta C_\psi & S_\Phi S_\theta C_\psi - C_\Phi S_\psi & C_\Phi S_\theta C_\psi + S_\Phi S_\psi \\ C_\theta S_\psi & S_\Phi S_\theta S_\psi + C_\Phi C_\psi & C_\Phi S_\theta S_\psi - S_\Phi C_\psi \\ -S_\theta & S_\Phi C_\theta & C_\Phi C_\theta \end{bmatrix} \tag{15}$$

where $S_\Phi \equiv \sin(\Phi)$, $C_\Phi \equiv \cos(\Phi)$, $S_\theta \equiv \sin(\theta)$, $C_\theta \equiv \cos(\theta)$, $S_\psi \equiv \sin(\psi)$, and $C_\psi \equiv \cos(\psi)$.

(2) Quaternion: A quaternion is a four-dimensional extension to complex numbers, containing four real parameters. The first is considered a scalar and the other three vector components in three-dimensional space. It is written as $\mathbf{q} = e_0 + e_1 i + e_2 j + e_3 k$. Unlike the DCM, the relations between the quaternion of rotation $\mathbf{q}$ and the two vectors $\mathbf{f}^b$ and $\mathbf{f}^n$ are nonlinear.

There are four parameters used to describe the orientation while only three are necessary, where a constant equation exists of the form

$$e_0^2 + e_1^2 + e_2^2 + e_3^2 = 1$$

These equations have advantages over the equivalent Euler angle based transformation, since

1. They apply to all attitudes.
2. The error equations are bounded by the constraint equation.
3. The numerical value of each parameter always lies in the range -1 to 1, so that the scaling problems in the computing mechanization can be easily handled.

The rotation matrix in terms of the unit quaternion parameters $\mathbf{q}_b^n$ can be written as

$$\mathbf{q}_b^n = \begin{bmatrix} e_0^2 + e_1^2 - e_2^2 - e_3^2 & 2(e_1 e_2 - e_0 e_3) & 2(e_1 e_3 + e_0 e_2) \\ 2(e_1 e_2 + e_0 e_3) & e_0^2 + e_1^2 - e_2^2 - e_3^2 & 2(e_2 e_3 - e_0 e_1) \\ 2(e_1 e_3 - e_0 e_2) & 2(e_2 e_3 + e_0 e_1) & e_0^2 + e_3^2 - e_1^2 - e_2^2 \end{bmatrix}$$

(16)

where $e_0 \sim e_3$ are the quaternion vector components. The following relationships with Euler angles can be derived [10]

$$\sin \theta = 2(e_0 e_2 - e_3 e_1)$$

$$\tan \psi = \frac{2(e_0 e_3 + e_1 e_2)}{e_0^2 + e_1^2 - e_2^2 - e_3^2}$$

$$\tan \Phi = \frac{2(e_0 e_1 + e_2 e_3)}{e_0^2 - e_1^2 - e_2^2 + e_3^2}$$

(17)

It can be shown that

$$\begin{bmatrix} \dot{e}_0 \\ \dot{e}_1 \\ \dot{e}_2 \\ \dot{e}_3 \end{bmatrix} = \begin{bmatrix} -e_1 & -e_2 & -e_3 \\ e_0 & -e_3 & e_2 \\ e_3 & e_0 & -e_1 \\ e_2 & e_1 & e_0 \end{bmatrix} \begin{bmatrix} p \\ q \\ r \end{bmatrix}$$
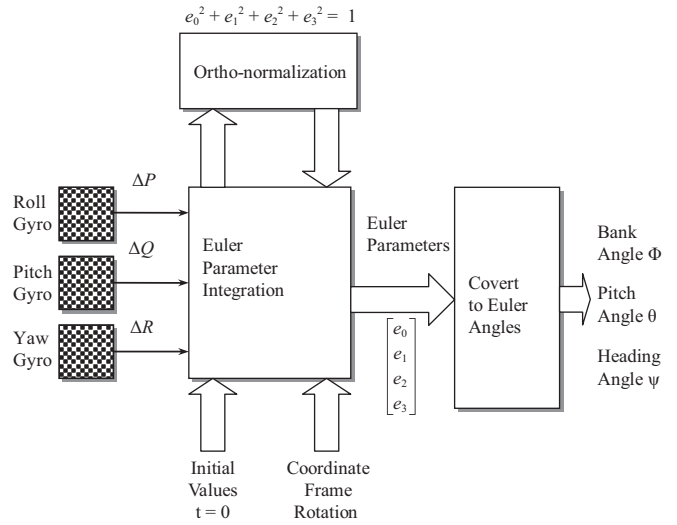
(18)

which can be re-arranged into the form

Fig. 4. Attitude derivation using the quaternion [10].

$$\begin{bmatrix} \dot{e}_0 \\ \dot{e}_1 \\ \dot{e}_2 \\ \dot{e}_3 \end{bmatrix} = 1/2 \begin{bmatrix} 0 & -p & -q & -r \\ p & 0 & r & -q \\ q & -r & 0 & p \\ r & q & -p & 0 \end{bmatrix} \begin{bmatrix} e_0 \\ e_1 \\ e_2 \\ e_3 \end{bmatrix}$$

(19)

The quaternion is propagated according to the differential equation

$$\dot{\mathbf{q}} = \frac{1}{2} \mathbf{\Omega}(\omega_{nb}^b) \mathbf{q}$$

(20)

where $\mathbf{q} = [e_0 \quad e_1 \quad e_2 \quad e_3]^T$ denotes the quaternion vector, and $\omega_{nb}^b = [p \quad q \quad r]^T$ denotes the body angular rate vector. Fig. 4 provides the attitude derivation using the quaternion [10].

IV. CALCULATION OF THE ACCELEROMETER AND GYRO OUTPUTS

The specific forces and angular rates are used as inputs to the navigation algorithms. The numerical simulator used for generating the input data of the specific forces was developed by solving the navigation equation expressed in *n* frame

$$\mathbf{f}^n = \dot{\mathbf{V}}^n + [\mathbf{\Omega}(\omega_{en}^n) + 2\mathbf{\Omega}(\omega_{ie}^n)]\mathbf{V}^n - \mathbf{g}_l^n$$

(21)

Fig. 5 shows the algorithm for generating the measured vehicle angular rates and specific forces. The flow chart for calculation of the accelerometer and gyro outputs is shown as in Fig. 6 [1]. An alternative methods for generating the body angular rates and specific forces using the INS Toolbox by GPSoft LLC [3] is shown in Fig. 7.
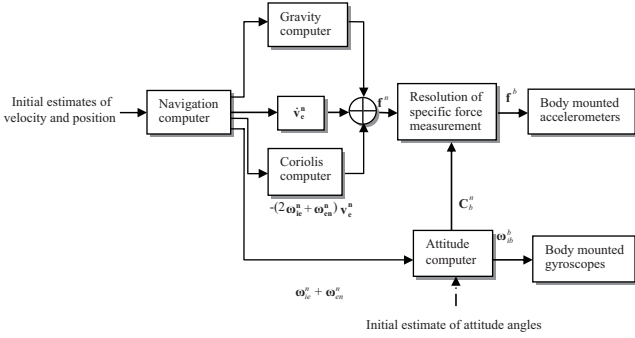
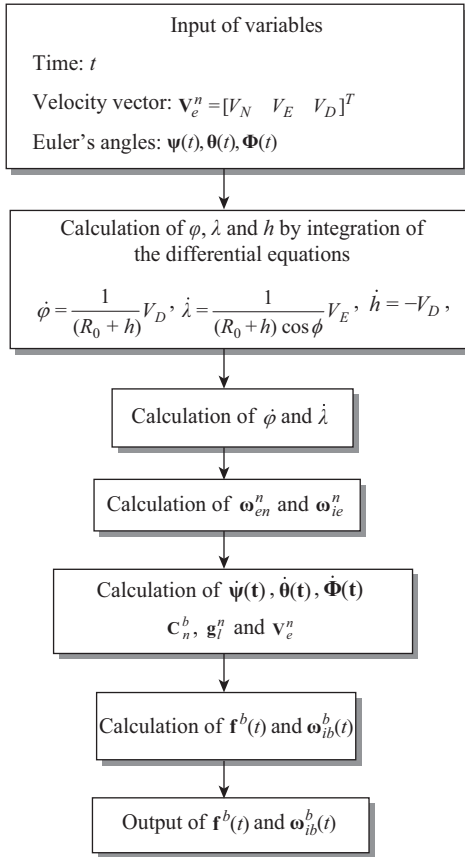**Fig. 5. The block diagram for generating accelerometer and gyroscope outputs in a SINS mechanization.**

Fig. 7. The block diagram for generating the body angular rates and specific forces using the INS toolbox.

Input of variables

Time: t

Velocity vector: $\mathbf{V}_e^n = [V_N \quad V_E \quad V_D]^T$

Euler's angles: $\psi(t), \theta(t), \Phi(t)$

Calculation of φ, λ and h by integration of the differential equations

$\dot{\varphi} = \dfrac{1}{(R_0 + h)} V_D$, $\dot{\lambda} = \dfrac{1}{(R_0 + h)\cos\phi} V_E$, $\dot{h} = -V_D$,

---

Calculation of $\dot{\varphi}$ and $\dot{\lambda}$

Calculation of $\boldsymbol{\omega}_{en}^n$ and $\boldsymbol{\omega}_{ie}^n$

Calculation of $\dot{\psi}(t), \dot{\theta}(t), \dot{\Phi}(t)$
$\mathbf{C}_n^b$, $\mathbf{g}_l^n$ and $\mathbf{V}_e^n$

Calculation of $\mathbf{f}^b(t)$ and $\boldsymbol{\omega}_{ib}^b(t)$

Output of $\mathbf{f}^b(t)$ and $\boldsymbol{\omega}_{ib}^b(t)$

Fig. 6. Flow chart for calculation of the accelerometer and gyro outputs.

V. ILLUSTRATIVE EXAMPLES

Several tests have been implemented to confirm the validity of the simulation platform. The fourth order Runge-Kutta (RK) integration method is employed for solving the equations.

(1) Example 1 - the ballistic trajectory [1]

An example on the ballistic trajectory, as shown in Fig. 8, is presented as the first example. In the case of a pure ballistic trajectory, the gravitational acceleration is constant and the specific forces equal zero. The angular rate is produced only
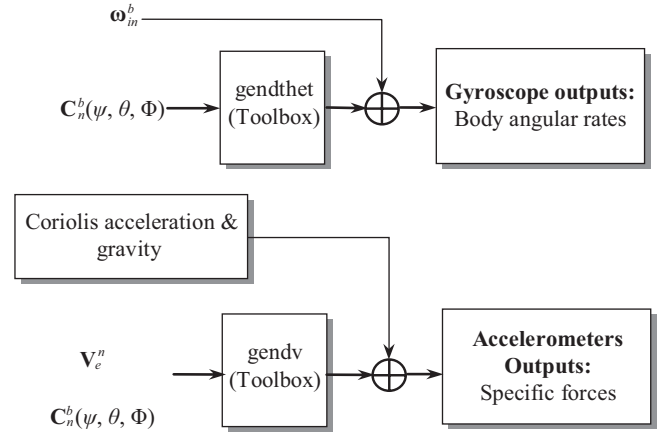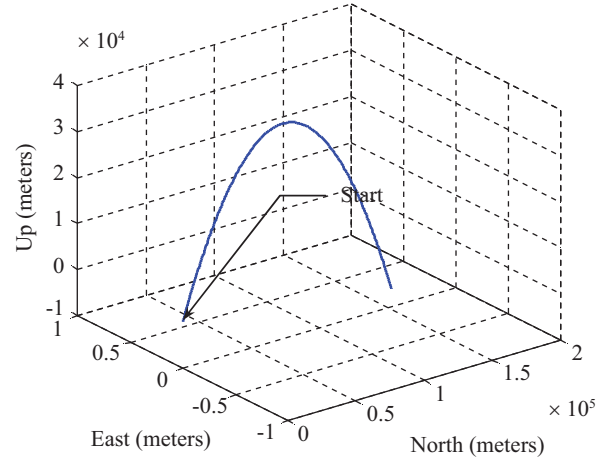

Fig. 8. The ballistic trajectory.

in pitch plane due to the gravity. It should be mentioned that for solving navigation equations the gravitational acceleration is variable and it depends on the altitude. Also there is the effect of Coriolis acceleration due to Earth rotation. Therefore, in order to produce a pure ballistic trajectory in the navigation frame under these conditions it is necessary to generate specific force and angular rate to compensate variable gravitational and the Coriolis accelerations. The body angular rate components for this example are shown in Fig. 9; the specific force profiles are shown in Fig. 10.

This example represents a simple motion where the object has a pure ballistic trajectory without any disturbance and with the gravitational acceleration which is equal to $g = 9.81 \, m/s^2$. The velocity vector in North, East and Down directions is given by

$$\mathbf{V}_e^n = \begin{bmatrix} V_N \\ V_E \\ V_D \end{bmatrix} = \begin{bmatrix} V_0 \cos\theta_0 \\ 0 \\ -(V_0 \sin\theta_0 - gt) \end{bmatrix} \tag{22}$$
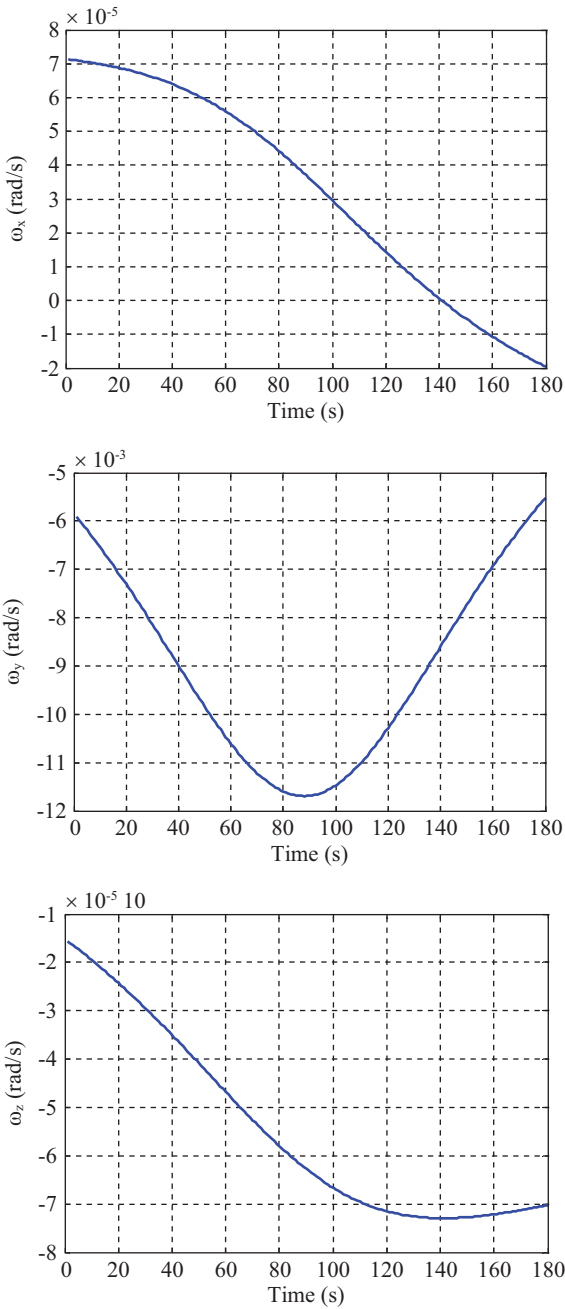
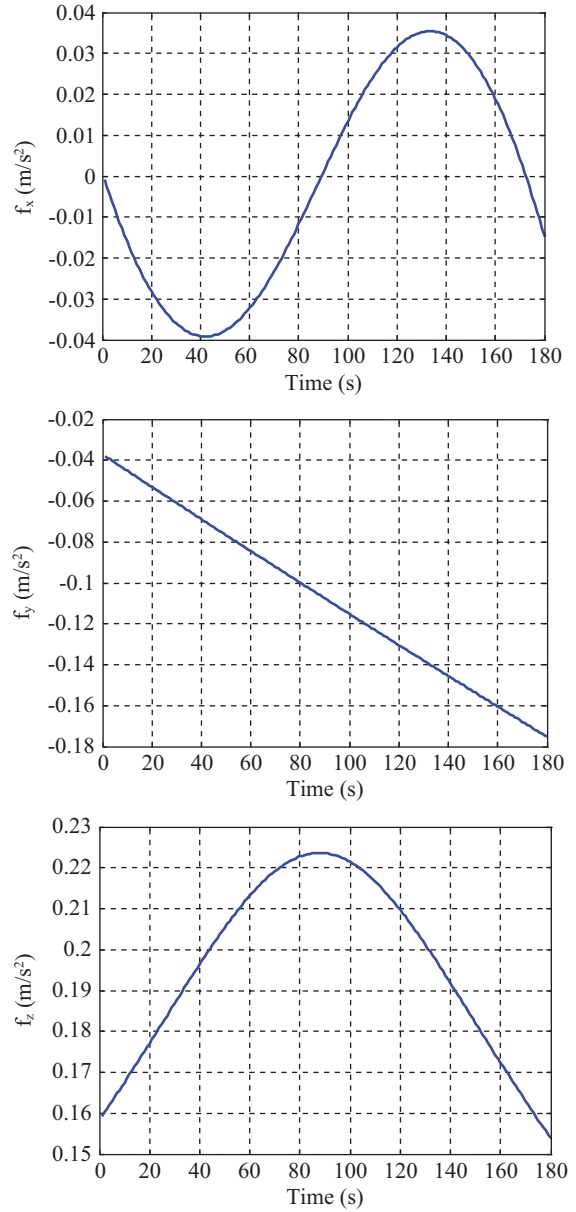Fig. 9. Body angular rate components - the ballistic trajectory.

Fig. 10. Specific force profiles - the ballistic trajectory.

$$\psi = \dot{\psi} = 0; \; \Phi = \dot{\Phi} = 0$$

The first derivative of the velocity vector is

$$\dot{\mathbf{V}}_e^n = \begin{bmatrix} \dot{V}_N \\ \dot{V}_E \\ \dot{V}_D \end{bmatrix} = \begin{bmatrix} 0 \\ 0 \\ g \end{bmatrix} \quad (23)$$

The calculated numerical value of the initial velocity is 1200 m/*s*. The initial latitude, longitude and altitude are: $\phi_0 = 1$ radian, $\lambda_0 = 0$ and $h_0 = 0$ m. The values of the yaw and roll angles and their derivatives are set to equal zero

The numerical value for the launch angle $\theta_0 = 45°$ was selected to have maximum down range. The derivative of the pitch angle is obtained as

$$\dot{\theta} = -\frac{g}{V_0 \cos\theta_0} \cos^2\theta \quad (24)$$

(2) Example 2- the 2D automobile trajectory

The following three examples are adopted from the INS Toolbox [3]. Fig. 11 shows the 2D automobile trajectory where pitch and roll are assumed to stay constant at zero degrees and

Table 1. Description of the motion for the 2D automobile trajectory (initial position: [0, 0, 0 meters] in NED frame).

Segment number	Description of the motion
1	Level acceleration to 30 m/s
2	Straight for 61 sec
3	Turn right 90 degrees
4	Straight for 61 sec
5	Turn right 90 degrees
6	Straight for 61 sec
7	180 degree turn
8	Straight for 61 sec
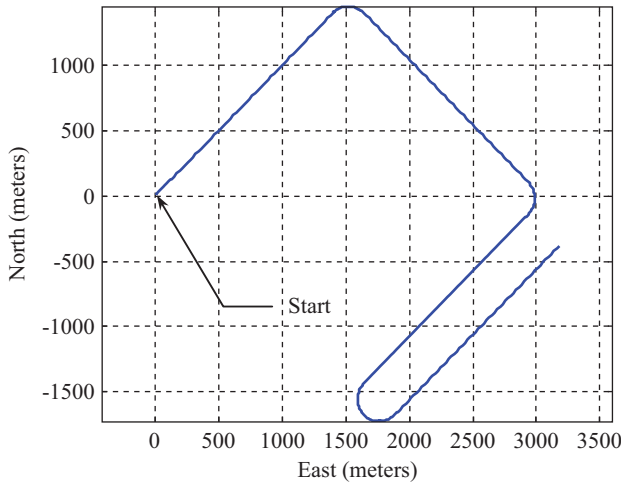
Fig. 11. The 2D automobile trajectory.

the yaw angle follows the heading of the vehicle. The level paths consists of straight segments and constant-radius turns. The results are generated in an east-north-up coordinate system. The INS toolbox can also be employed to generate the simplified 2D automobile trajectory. Description of the motion for the 2D automobile trajectory is summarized in Table 1. The body angular rate components and specific force profiles are depicted in Fig. 12 and Fig. 13, respectively.

(3) Example 3 - the 3D simple flight path

Adopted from the INS toolbox [3], the 3D simple flight path is shown as in Fig. 14. Table 2 provides the description of the motion for the flight path. The body angular rates and specific force profiles for this example are depicted in Fig. 15 and Fig. 16, respectively.

(4) Example 4 - F-16 flight trajectory

The F-16 flight trajectory shown in Fig. 17 is also adopted from the INS toolbox. Description of the motion for the F-16 flight trajectory is summarized in Table 3. The body angular rates and specific force profiles for the F-16 flight are depicted in Fig. 18 and Fig. 19, respectively.
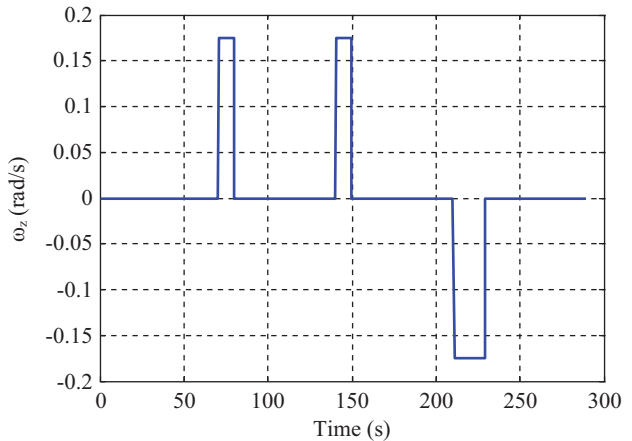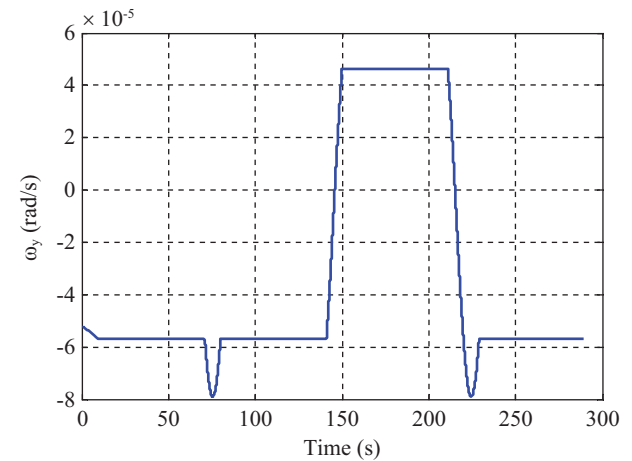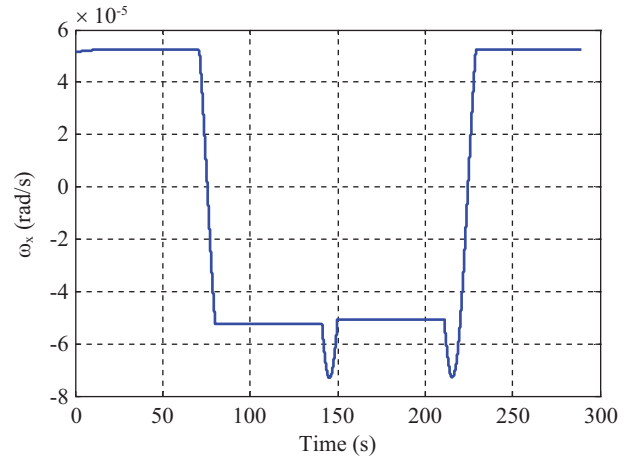
Fig. 12. Body angular rate components - the 2D automobile trajectory.

(5) Example 5 – Another 3D flight trajectory

For this example, a 3D flight trajectory designed by the authors is presented. In the example, 10 segments involving time-varying dynamic characteristics are arranged, as shown in Fig. 20. Description of the motion for the 3D flight trajectory is summarized in Table 4. The corresponding body angular body rates and specific force profiles for the motion are depicted in Fig. 21 and Fig. 22, respectively.
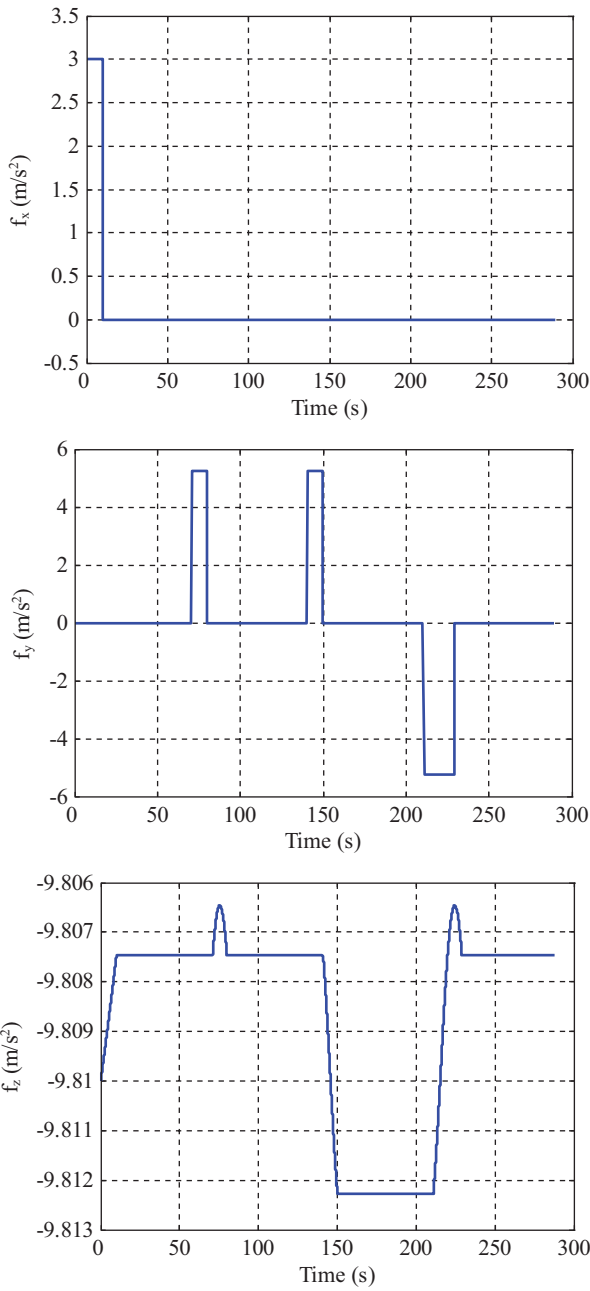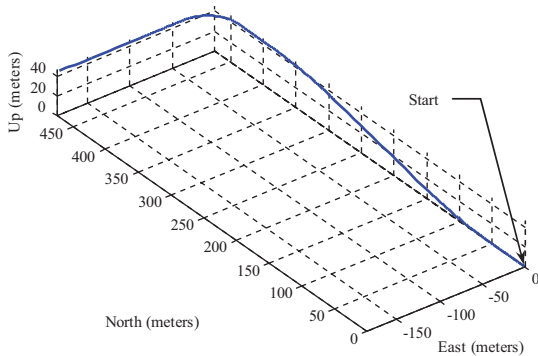
Table 2. Description of the motion for the 3D simple flight path (initial position: [0, 0, 0 meters] in NED frame).

Segment number	Description of the motion
1	Level acceleration for 10 seconds
2	Pitch up transition
3	15 second climb
4	Level off
5	Roll into a turn
6	90 degree turn
7	Roll back to straight and level
8	10 second straight segment to the West

Fig. 13. Specific force profiles - the 2D automobile trajectory.

Fig. 14. The 3D simple flight path.
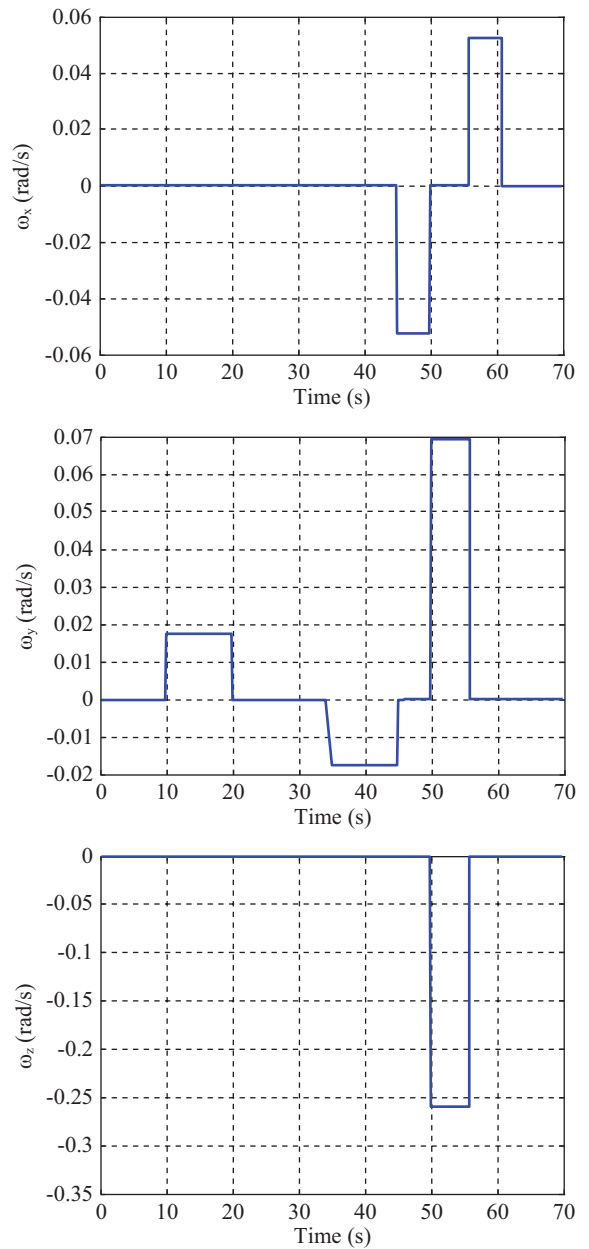
Fig. 15. Body angular rate components - the 3D simple flight path.

Table 3. Description of the motion for the F-16 flight trajectory (initial position: [200, 100, -50 meters] in NED frame).

Segment number	Description of the motion
1	Level acceleration for 20 seconds up to 75 m/s
2	Level acceleration up to 200 m/s
3	15 degree climb up to an altitude of 2500 meters
4	Straight-and-level flight for 10 seconds
5	Left turn at 3 deg/sec to a heading of 270 degrees
6	Straight-and-level flight for 10 seconds
7	20 degree descent down to an altitude of 1500 meters
8	Straight-and-level flight for 20 seconds

Fig. 16. Specific force profiles - the 3D simple flight path.

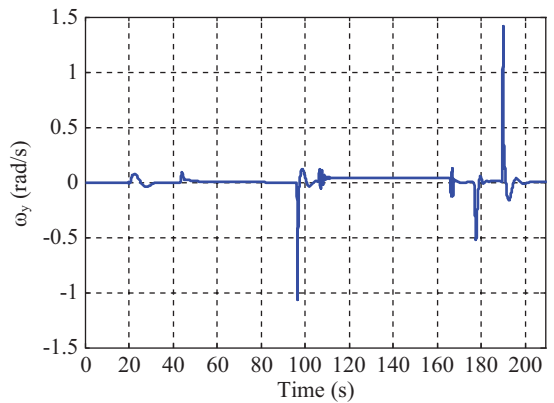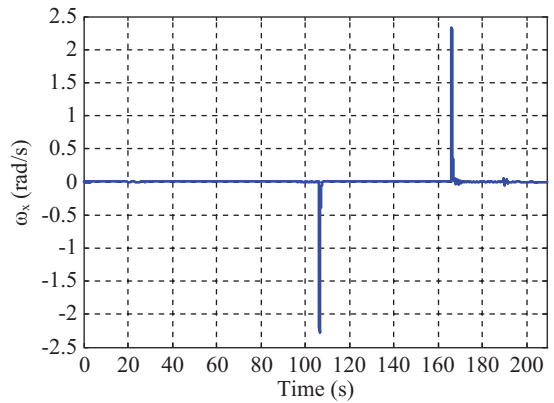**Fig. 17. F-16 flight trajectory.**
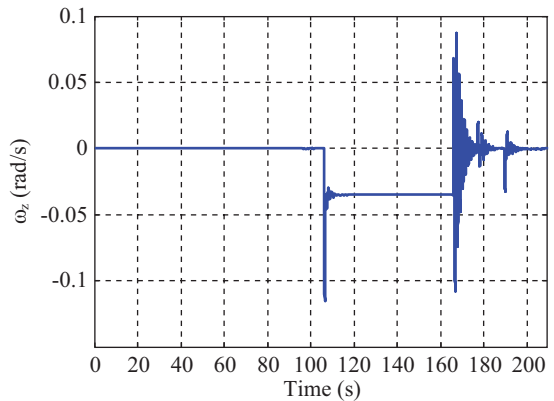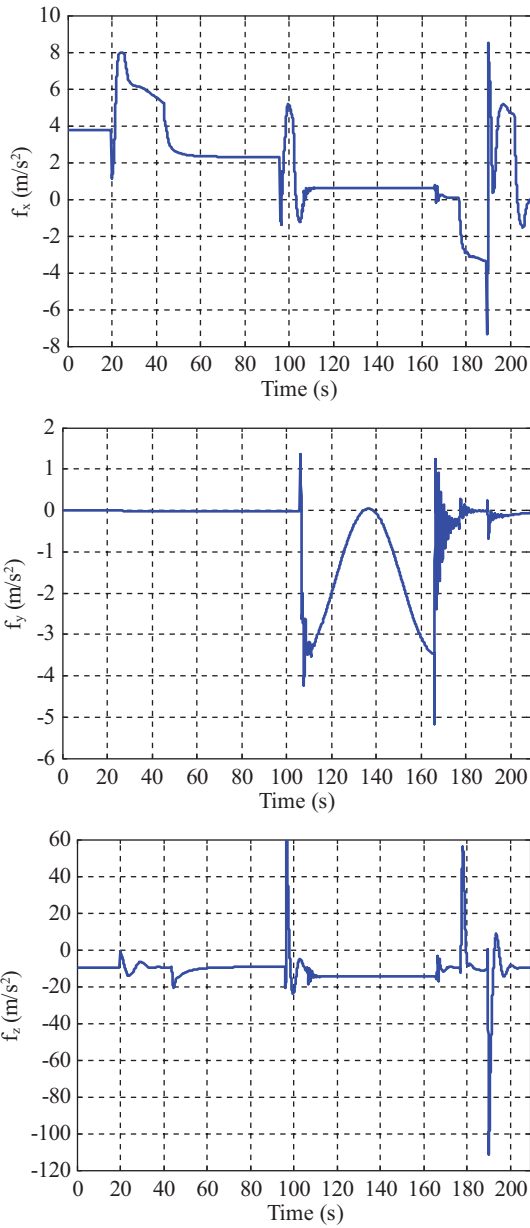

Fig. 18. Body angular rate components - F-16 flight trajectory.

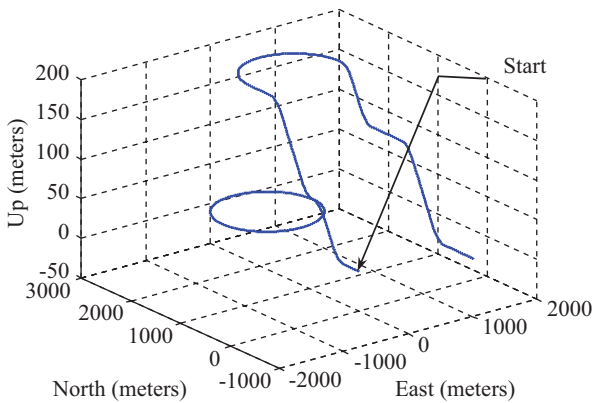**Fig. 19. Specific force profiles - F-16 flight trajectory.**

Fig. 20. 3D flight trajectory.

Table 4. Description of the motion for the 3D flight trajectory given in Example 5 (initial position: [0, 0, 0 meters] in NED frame).

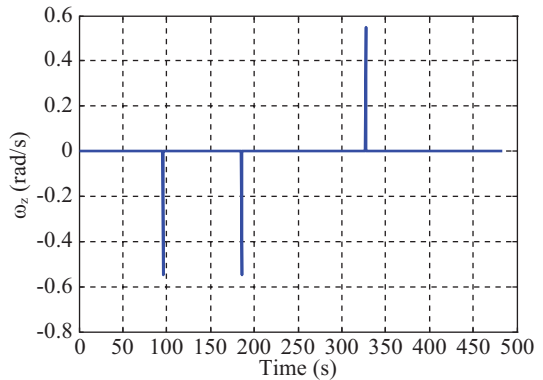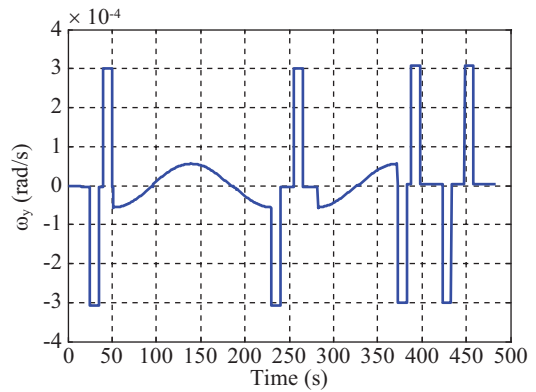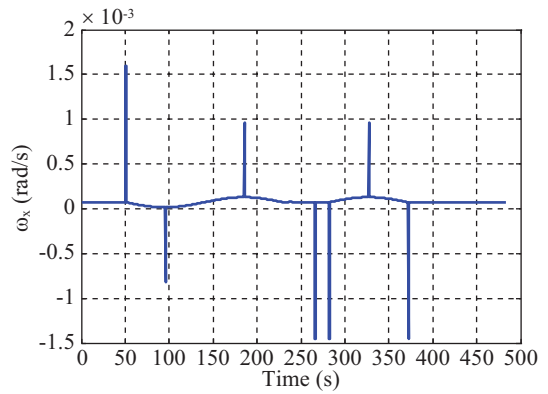| Segment number	Description of the motion
1	Constant acceleration level flight
2	Climbing
3	Counter-clockwise circular motion
4	Climbing
5	Constant velocity level flight
6	Constant acceleration clockwise turn
7	Descending
8	Constant velocity level flight
9	Descending
10	Constant velocity level flight

Fig. 21. Body angular rate components - 3D flight trajectory for Example 5.
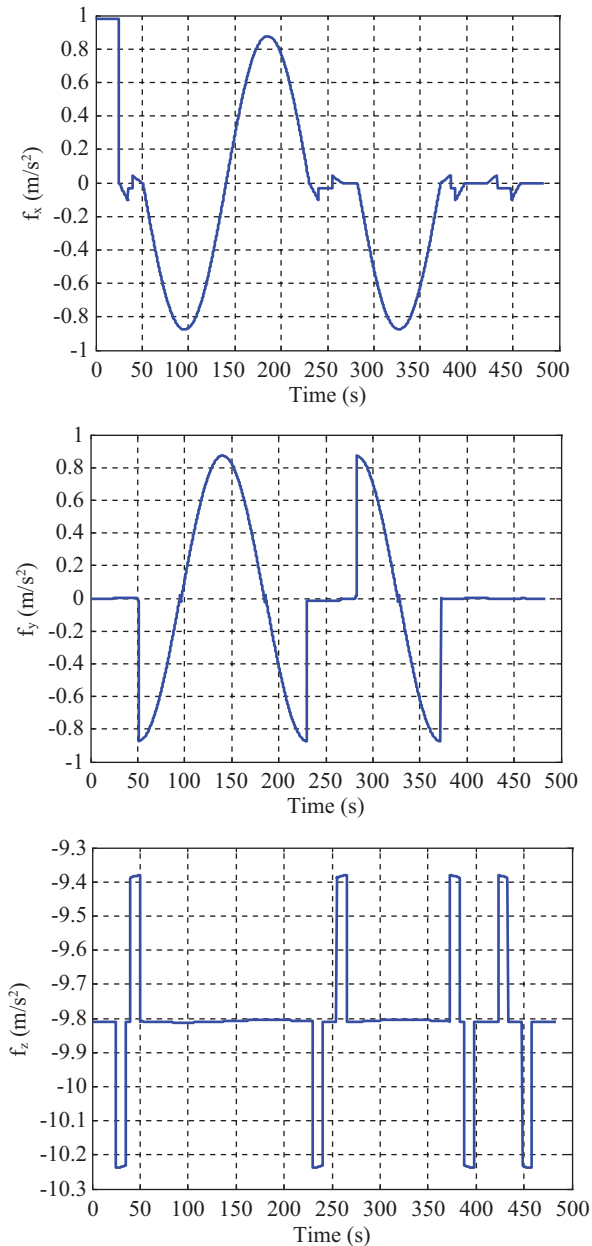
Fig. 22. Specific force profiles - 3D flight trajectory for Example 5.

VI. CONCLUSIONS

This paper presents a strapdown inertial navigation system (SINS) simulation platform. The numerical simulator solves the navigation equations in navigation frame where the quaternion vector is employed for attitude calculation. Five examples were presented to examine the simulator. These examples covered a wide variety of dynamic characteristics, including the ballistic trajectory, the 2D automobile trajectory, the 3D simple flight path, the F-16 flight trajectory, and a more complicated 3D flight trajectory. The results confirm the validity of the simulation platform and provide the readers with further information for developing their own SINS simulation tool.

REFERENCES

1. Ahmed, M. S. and Cuk, D. V., "Comparison of different computation methods for strapdown inertial navigation systems," *Scientific Technical Review*, Vol. LV, No. 2, pp. 22-29 (2005).
2. Bar-Itzhack, I. Y., "Navigation computation in terrestrial strapdown inertial navigation systems," *IEEE Transactions on Aerospace and Electronic Systems*, Vol. AES-13, No. 6, pp. 679-689 (1977).
3. GPSoft LLC, *Inertial Navigation System TOOLBOX 3.0 User's Manual* (2007).
4. Jekeli, C., *Inertial Navigation Systems with Geodetic Applications*, Walter de Gruyter (2000).
5. Kayton, M. and Fried, W., *Avionics Navigation Systems*, 2nd Edition, John Wiley & Sons (1997).
6. Peng, S. and Zhang, B., "Study on attitude updating algorithm of SINS," *2011 International Conference on Electronics and Optoelectronics*, Vol. 4, pp. 49-52 (2011).
7. Savage, P., *Introduction to Strapdown Inertial Navigation Systems*, 8th Printing, Strapdown Associates, Inc. (1997).
8. Savage, P., "Strapdown inertial navigation integration algorithm design part 1: Attitude algorithms," *AIAA Journal of Guidance, Control and Dynamics*, Vol. 21, No. 1, pp. 19-28 (1998).
9. Savage, P., "Strapdown inertial navigation integration algorithm design part 2: Velocity and position algorithms," *AIAA Journal of Guidance, Control and Dynamics*, Vol. 21, No. 2, pp. 208-221 (1998).
10. Collinson, P. R. G., *Introduction to Avionics*, Chapman & Hall. (1995).
11. Titterton, D. and Weston, J., *Strapdown Inertial Navigation Technology*, 2nd Edition, Progress in Astronautics and Aeronautics Series, Volume 207, AIAA on behalf of the Institution of Electrical Engineers, pp. 295-297 (2004).
12. Zhang, W., Ghogho, M., and Yuan, B., "Mathematical model and simulation of strapdown inertial navigation system," *Modelling and Simulation in Engineering*, Vol. 2012, pp. 1-25 (2012).